ANALYSIS OF CABLE SUPPORTED STRUCTURE CONSIDERING CABLE SLIDING

Chung, Kwang Sup
Deputy General Manager,
POSCO E&C
cksupi@empal.com

Park, Jung Il
Vice President
Cheil Engineering Co.
Seoul, Korea
ilsim001@snu.ac.kr

Chang, Sung-Pil
Professor Emeritus
Seoul Nat'l University
Seoul, Korea
spchang@snu.ac.kr

Abstract: *The goal of this study is to develop a 3-dimensional elastic cable finite element which considers the sliding effect and uses the geometric nonlinear cable finite element based on elastic catenary theory. In this study, two types of sliding were considered: the roller sliding condition without friction and the frictional sliding condition. These were formulated to derive the nodal force vectors and tangential stiffness matrices. To validate the proposed 3-dimensional cable sliding element, experiments were conducted for both sliding conditions, and compared to calculations of the amount of sliding and displacement at the loading point. Overall calculations using the 3-dimensional cable sliding model were in very good agreement with the measured values.*

Keywords: cable finite element; elastic catenary; roller sliding; frictional sliding; cable sliding

1. INTRODUCTION

The purpose of this study is to develop a 3-dimensional elastic cable finite element which considers the sliding effect of cables. This was achieved using the geometric nonlinear cable finite element based on elastic catenary theory. The elastic catenary cable finite element on the vertical cable plane was developed by Chang and Park [1], and is based on the well known elastic catenary cable theory [2] and employed in the spatial modeling of cable members through a simple coordinate transformation on the horizontal plane [3]. Ahn [4] and Park [5] formulated the 3-dimensional profile expressions of an elastic catenary cable element subjected to self-weight only. Until recently, continuous model updates have been performed by the Seoul National University [6,7], but the model still does not take into account the cable sliding effect.
Recently, a multi-node cable element allowing sliding without friction at its nodes has been developed by Kim et al. [8]. A two-node truss element was extended to a multi-node truss element which maintains constant tension but is connected through several nodes without friction. However, its tangential stiffness is derived under the linear elastic condition and assumes that the cable is straight before and after deformation occurs. This research was originally planned for application to the external pre-stressing method using strands based on Troitsky's theory [9].
`In this paper, two types of sliding were considered: the roller sliding condition without friction and the frictional sliding condition. These were formulated to derive the nodal force vectors and tangential

stiffness matrices. To validate the 3-dimensional cable sliding element developed here, experiments representing both sliding conditions were conducted and compared with calculations of the amount of sliding at the saddle and the displacement at the loading point.
This paper describes the formulation of the cable sliding problem using the elastic catenary cable element. In addition, a simplified cable-supported structural system was analyzed to investigate the characteristics of a realistic structure with cable sliding but this result can be seen in reference [10].

2. NUMERICAL FORMULATION OF CABLE SLIDING

2.1 Local nodal displacement and force vector

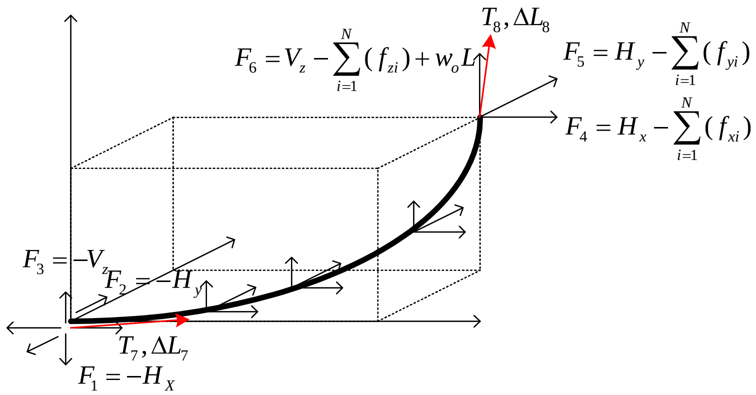

(a) Roller sliding condition

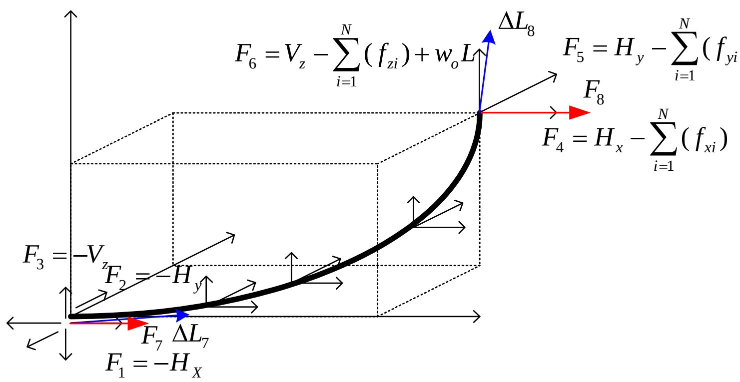

(b) Frictional sliding condition

Figure 1: 3-Dimensional elastic catenary cable element

This study classifies an instance of cable sliding as either roller sliding without friction, or as frictional sliding. Figure 1(a) and (b) show elastic catenary cable elements which consider roller sliding and frictional sliding, respectively. When defining the nodal force vector, which is a nonlinear function of displacement, the nodal force due to the length of cable sliding is added to the nodal force vector due to the nodal displacement.

When both roller and frictional sliding (Figure 1) are compared with the element that does not consider the sliding effect, the cable length L becomes $L_0 + \Delta L_7 - \Delta L_8$. That is, the sliding effect leads to a change in length (unstrained length L_0; length lengthening $+\Delta L_7$; length shortening $-\Delta L_8$) (See Figure 1). For sliding conditions, the element's local nodal displacement Δ and force vector F_Δ can be defined as follows,

$$\Delta = \{\Delta_1, \Delta_2, \Delta_3, \Delta_4, \Delta_5, \Delta_6, \Delta L_7, \Delta L_8\}^T \tag{1}$$

$$\begin{aligned} F_\Delta &= \{F_1, F_2, F_3, F_4, F_5, F_6, F_7, F_8\}^T \\ &= \left\{ -H_x,\ -H_{y,}\ -V_z,\ H_x - \sum_{j=1}^{N}(f_{xj}),\ H_y - \sum_{j=1}^{N}(f_{yj}),\ V_z - \sum_{j=1}^{N}(f_{zj}) + w_o L,\ F_7,\ F_8 \right\}^T \end{aligned} \tag{2}$$

where for roller sliding

$$F_7 = \sqrt{H_x^2 + H_y^2 + V_z^2} \tag{3a}$$

$$F_8 = -\sqrt{\left(H_x - \sum_{j=1}^{N}(f_{xj})\right)^2 + \left(H_y - \sum_{j=1}^{N}(f_{yj})\right)^2 + \left(V_z - \sum_{j=1}^{N}(f_{zj}) + w_o L\right)^2} \tag{4a}$$

and for frictional sliding

$$F_7 = -H_x + \beta(H_y + V_z) \tag{3b}$$

$$F_8 = \left(H_x - \sum_{j=1}^{N}(f_{xj})\right) + \beta\left\{\left(H_y - \sum_{j=1}^{N}(f_{yj})\right) + \left(V_z - \sum_{j=1}^{N}(f_{zj}) + w_o L\right)\right\} \tag{4b}$$

2.2 Geometrical compatibility equations

The geometric compatibility equation, which is a nonlinear function of cable element force, is also defined by the parameter of cable sliding length. The geometric compatibility conditions can be defined as in the following equation for both roller and frictional sliding:

$$\begin{aligned} X(S_{N+1}) &= l_x = l_{x0} - \Delta_1 + \Delta_4 = f(H_x, H_y, V_z, L_0 + \Delta L_7 - \Delta L_8) \\ Y(S_{N+1}) &= l_y = l_{y0} - \Delta_2 + \Delta_5 = g(H_x, H_y, V_z, L_0 + \Delta L_7 - \Delta L_8) \\ Z(S_{N+1}) &= l_z = l_{z0} - \Delta_3 + \Delta_6 = h(H_x, H_y, V_z, L_0 + \Delta L_7 - \Delta L_8) \end{aligned} \tag{5}$$

2.3 Derivation of tangential stiffness matrix

The element tangential stiffness matrix element was defined based on elastic catenary theory as in Eq. (6), and each component was derived separately in five groups as indicated.

$$\frac{dF_\Delta}{d\Delta}=\begin{bmatrix}\frac{dF_1}{d\Delta_1} & \frac{dF_1}{d\Delta_2} & \frac{dF_1}{d\Delta_3} & \frac{dF_1}{d\Delta_4} & \frac{dF_1}{d\Delta_5} & \frac{dF_1}{d\Delta_6} & \frac{dF_1}{d\Delta L_7} & \frac{dF_1}{d\Delta L_8} \\ \frac{dF_2}{d\Delta_1} & \frac{dF_2}{d\Delta_2} & \frac{dF_2}{d\Delta_3} & \frac{dF_2}{d\Delta_4} & \frac{dF_2}{d\Delta_5} & \frac{dF_2}{d\Delta_6} & \frac{dF_2}{d\Delta L_7} & \frac{dF_2}{d\Delta L_8} \\ \frac{dF_3}{d\Delta_1} & \frac{dF_3}{d\Delta_2} & \frac{dF_3}{d\Delta_3} & \frac{dF_3}{d\Delta_4} & \frac{dF_3}{d\Delta_5} & \frac{dF_3}{d\Delta_6} & \frac{dF_3}{d\Delta L_7} & \frac{dF_3}{d\Delta L_8} \\ \frac{dF_4}{d\Delta_1} & \frac{dF_4}{d\Delta_2} & \frac{dF_4}{d\Delta_3} & \frac{dF_4}{d\Delta_4} & \frac{dF_4}{d\Delta_5} & \frac{dF_4}{d\Delta_6} & \frac{dF_4}{d\Delta L_7} & \frac{dF_4}{d\Delta L_8} \\ \frac{dF_5}{d\Delta_1} & \frac{dF_5}{d\Delta_2} & \frac{dF_5}{d\Delta_3} & \frac{dF_5}{d\Delta_4} & \frac{dF_5}{d\Delta_5} & \frac{dF_5}{d\Delta_6} & \frac{dF_5}{d\Delta L_7} & \frac{dF_5}{d\Delta L_8} \\ \frac{dF_6}{d\Delta_1} & \frac{dF_6}{d\Delta_2} & \frac{dF_6}{d\Delta_3} & \frac{dF_6}{d\Delta_4} & \frac{dF_6}{d\Delta_5} & \frac{dF_6}{d\Delta_6} & \frac{dF_6}{d\Delta L_7} & \frac{dF_6}{d\Delta L_8} \\ \frac{dF_7}{d\Delta_1} & \frac{dF_7}{d\Delta_2} & \frac{dF_7}{d\Delta_3} & \frac{dF_7}{d\Delta_4} & \frac{dF_7}{d\Delta_5} & \frac{dF_7}{d\Delta_6} & \frac{dF_7}{d\Delta L_7} & \frac{dF_7}{d\Delta L_8} \\ \frac{dF_8}{d\Delta_1} & \frac{dF_8}{d\Delta_2} & \frac{dF_8}{d\Delta_3} & \frac{dF_8}{d\Delta_4} & \frac{dF_8}{d\Delta_5} & \frac{dF_8}{d\Delta_6} & \frac{dF_8}{d\Delta L_7} & \frac{dF_8}{d\Delta L_8}\end{bmatrix} \tag{6}$$

A major difference from the conventional elastic catenary element is found in the following components: $\left[\frac{dF_7}{d\Delta_j}\right]_{j=1,\cdots,6}$, $\left[\frac{dF_8}{d\Delta_j}\right]_{j=1,\cdots,6}$, and $\left[\frac{dF_i}{d\Delta L_j}\right]_{i,j=7,8}$. The procedure used to evaluate these components are described in reference [10].

3. Experimental verification

3.1 Experimental program

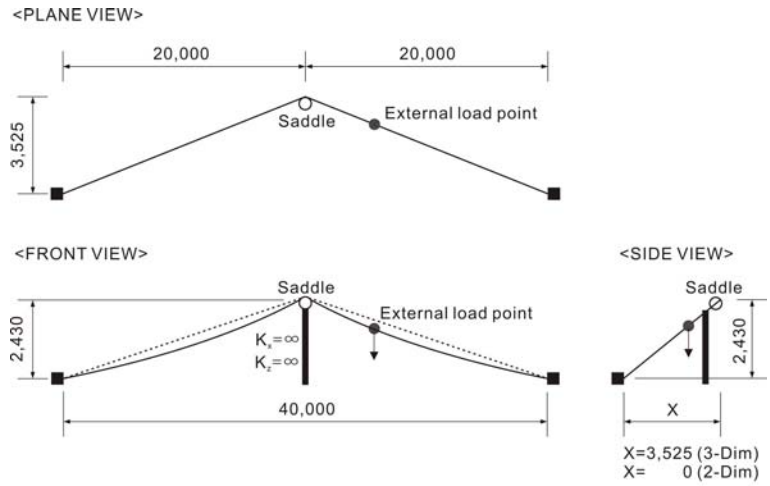

Figure 2: Test configuration (unit: mm)

A simple experiment was conducted to validate the element developed which included 2- and 3-dimensional roller and frictional sliding. Figure 2 show the test configuration employed in this test. The test model consisted of a wire with a 4 m long span, and a steel pylon with a height of 2,430 mm at the top of which a saddle system was mounted. Both ends of the wire were fixed at each support. In the 3-dimensional test model, the saddle was installed at the top of the pylon which deviated 3,525 mm from the center line at an angle of 35 degrees from the ground plane (See Figure 2). A roller bearing was employed to eliminate the friction effect.

The cable was modeled by a wire with diameter, cross-sectional area, and modulus of elasticity of 4.76 mm, 17.8 mm^2, and 195 GPa, respectively. Several external loading steps using balance weights were applied at quarter distances from the pylon. The cable sliding at the saddle and the vertical displacement at the loading point were measured using laser displacement measurement equipment.

3.2 Comparison with calculations

Table 1: Calculated and measured cable sliding length at saddle

Applied Load, [N]	Cable Sliding Length at Saddle, [mm]					
	Roller Sliding			Frictional Sliding		
	Calc. (1)	Meas. (2)	Ratio (1)/(2)	Calc. (3)	Meas. (4)	Ratio (3)/(4)
7.97	38.85	36.0	1.08	21.70	14.0	1.55
12.87	54.23	55.0	0.99	39.03	37.0	1.05
22.68	71.98	74.0	0.97	61.20	62.0	0.99
32.49	80.86	84.0	0.96	73.29	75.0	0.98
42.30	85.81	90.0	0.95	80.29	83.0	0.97
52.10	88.84	93.0	0.96	84.65	87.0	0.97

Table 2: Calculated and measured vertical displacement at loading point

Applied load, [N]	Vertical displacement at loading point, [mm]					
	Roller sliding			Frictional sliding		
	Calc. (1)	Meas. (2)	Ratio (1)/(2)	Calc. (3)	Meas. (4)	Ratio (3)/(4)
7.97	271.15	276.96	0.98	210.17	199.16	1.06
12.87	360.58	382.19	0.94	307.71	316.20	0.97
22.68	456.26	480.56	0.95	419.90	439.70	0.95
32.49	501.80	529.67	0.95	476.65	502.78	0.95
42.30	526.67	558.93	0.94	508.53	532.29	0.96
52.10	541.81	580.04	0.93	528.12	555.06	0.95

Elastic catenary cable element developed was validated through comparison with the experimental results found in this study. In calculations, the moving friction coefficient β was experimentally determined to be 0.25 for the materials used in this test. Table 1 and Figure 3 show a comparison of the measured and calculated sliding lengths at the saddle. Table 2 and Figure 4 show a comparison of the vertical displacement at the loading point. As seen in these tables and figures, roller sliding resulted in a larger sliding length at the saddle and a greater vertical displacement at the loading point than frictional sliding.

The calculated sliding length at the saddle was in good agreement with the measured values for both roller sliding and frictional sliding. The average calculated-to-measured ratio for roller sliding was 0.99

with a standard deviation of 0.05. The average calculated-to-measured ratio for frictional sliding was 1.09 with a standard deviation of 0.23. If the ratio of 1.55 at a relatively unstable initial loading step is disregarded, even better agreement can be expected (See Table 1 and Figure 3).

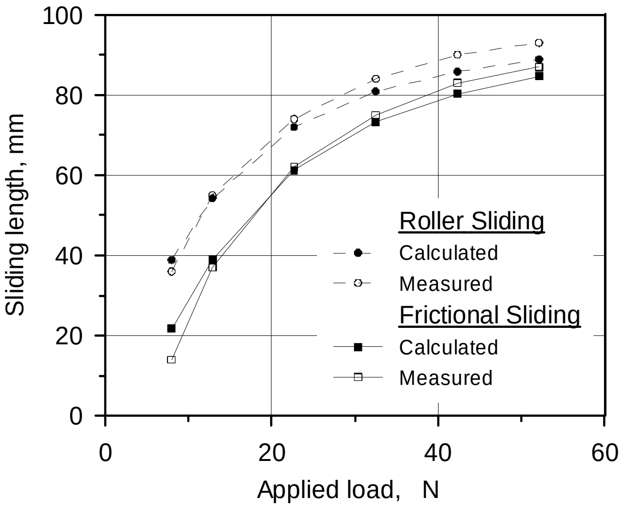

Figure 3: Comparison of calculated and measured sliding lengths at saddle

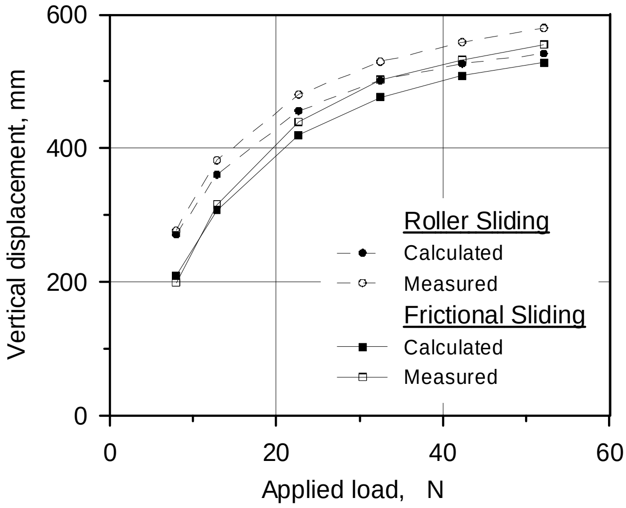

Figure 4: Comparison of calculated and measured vertical displacements at loading point

The calculated vertical displacement at the loading point was in good agreement with the measured values for both types of sliding. The average calculated-to-measured ratio for roller sliding was 0.95 with a standard deviation of 0.02, while for frictional sliding, the average calculated-to-measured ratio was 0.97 with a standard deviation of 0.04 (See Table 2 and Figure 4). As previously mentioned, 2-dimensional tests and numerical calculations were conducted and also showed good agreement.

4. CONCLUSIONS

A 3-dimensional, elastic catenary cable element which considers cable sliding is presented. This model is based on the theory of the geometric nonlinear cable finite element. Cable sliding is classified into two types: roller sliding without friction and frictional sliding. The element we developed was validated by comparing the measured and the calculated responses of a simple test model of a cable-supported structure. Based on our results, the following conclusions can be drawn:

The calculated sliding lengths at the saddle for both roller and frictional sliding were in good agreement with measured values. The average calculated-to-measured ratio for roller sliding was 0.99 with a standard deviation of 0.05, while for frictional sliding, the average calculated-to-measured ratio was 1.09 with a standard deviation of 0.23.

The calculated vertical displacements at the loading point for both roller and frictional sliding were also in good agreement with the measured values. The average calculated-to-measured ratio for roller sliding was 0.95 with a standard deviation of 0.02, while for frictional sliding, the average calculated-to-measured ratio was 0.97 with a standard deviation of 0.04.

In addition, a cable-supported structural system was analyzed to investigate the characteristics of a realistic structure with cable sliding. This result can be seen in reference [10]

The finite element presented here provides a useful tool for the nonlinear analysis and geometry control of cable-supported structures subjected to extreme loads such as earthquakes and strong winds.

REFERENCES

[1] Chang S. P. and Park J. I., “A Study on the Nonlinear Finite Cable Element.” Journal of Korean Society of Coastal and Ocean Engineers, Vol. 1, No. No.1, 1989, pp. 93-101.

[2] Irvine H. M., Cable Structures, MIT press, Cambridge, MA, 1981, pp. 15-24.

[3] Lee D. I., The Static Analysis of the Cable Member by FEM, MS thesis, Seoul Natl. Univ., Seoul, Korea, 1990.

[4] Ann S. S., Static and Dynamic Nonlinear Analysis of Spatial Cable Networks Using Elastic Catenary Cable Element, MS thesis, Seoul Natl. Univ., Seoul, Korea, 1991.

[5] Park Y. Y., Dynamic Analysis of Cable-suspended Roof System Subjected to a Wind Load, Doctoral thesis, Seoul Natl. Univ., Seoul, Korea, 1992.

[6] Park J. I., Lee K. C., and Chang S. P., “3D-elastic Catenary Cable Finite Element.” The 9th Korea–Japan Joint Seminar on Steel Bridges, Inha University, Incheon, Korea, 2007.

[7] Chang S. P., Park J. I., and Lee K. C., “Nonlinear Dynamic Analysis of Spatially Suspended Elastic Catenary Cable with Finite Element Method”, KSCE Journal of Civil Engineering, Vol. 12, No. 2, 2008, pp. 121-128.

[8] Kim M. Y., Lee J. S., Han M. Y., Kim S. B., and Kim, N. K., “A Multi-noded Cable Element Considering Sliding Effects.” The Journal of KSSC, Vol. 17, No.4, 2005, pp. 449-457.

[9] Troitsky M. S., Prestressed Steel Bridge: Theory and Design, Van Nostrand Reinhold, 1990.

[10] Chung K. S., 3 Dimensional Elastic Catenary Cable Element Considering Sliding Effect, Doctoral thesis, Seoul Natl. Univ., Seoul, Korea, 2008